

Lawrence Berkeley National Laboratory

Recent Work

Title

Efficient generation of sub-100 eV high-order harmonics from carbon molecules using infrared laser pulses

Permalink

<https://escholarship.org/uc/item/8qx5m02q>

Journal

Applied Physics Letters, 108(12)

ISSN

0003-6951

Authors

Fareed, MA
Thiré, N
Mondal, S
[et al.](#)

Publication Date

2016-03-21

DOI



10.1063/1.4944640

Peer reviewed

Efficient generation of sub-100 eV high-order harmonics from carbon molecules using infrared laser pulses

Cite as: Appl. Phys. Lett. **108**, 124104 (2016); <https://doi.org/10.1063/1.4944640>

Submitted: 22 February 2016 . Accepted: 09 March 2016 . Published Online: 22 March 2016

M. A. Fareed , N. Thiré , S. Mondal, B. E. Schmidt, F. Légaré, and T. Ozaki



View Online



Export Citation



CrossMark

ARTICLES YOU MAY BE INTERESTED IN

[A high-flux high-order harmonic source](#)

Review of Scientific Instruments **84**, 073103 (2013); <https://doi.org/10.1063/1.4812266>

[0.42TW 2-cycle pulses at 1.8 \$\mu\$ m via hollow-core fiber compression](#)

Applied Physics Letters **107**, 181101 (2015); <https://doi.org/10.1063/1.4934861>

[10 mJ 5-cycle pulses at 1.8 \$\mu\$ m through optical parametric amplification](#)

Applied Physics Letters **106**, 091110 (2015); <https://doi.org/10.1063/1.4914344>



Lake Shore
CRYOTRONICS

8600 Series VSM

For fast, highly sensitive
measurement performance

[LEARN MORE](#) 

2017
**R&D
100
WINNER**

Efficient generation of sub-100 eV high-order harmonics from carbon molecules using infrared laser pulses

M. A. Fareed, N. Thiré, S. Mondal, B. E. Schmidt, F. Légaré, and T. Ozaki^{a)}

Institut National de la Recherche Scientifique—Centre Énergie, Matériaux Télécommunications, 1650 boul. Lionel-Boulet, Varennes, Québec J3X 1S2, Canada

(Received 22 February 2016; accepted 9 March 2016; published online 22 March 2016)

We demonstrate broad bandwidth and intense sub-100 eV high-order harmonics from diatomic carbon molecules driven by long-wavelength laser pulses. Up to now, one limitation of the intense carbon harmonic source driven by a 0.8 μm wavelength Ti:sapphire laser has been the low cutoff around ~ 32 eV. In this paper, we show that this harmonic cutoff is extended to ~ 70 eV by increasing the driving laser wavelength to 1.71 μm . Surprisingly, the carbon harmonic intensity is found to be high despite the long wavelength driving laser. Experiments show only $\sim 30\%$ decrease in the harmonic intensity when changing the driving laser wavelength from 0.8 μm to 1.71 μm . Such intense sub-100 eV coherent X-rays would have important applications in various domains of science and technology. © 2016 AIP Publishing LLC. [<http://dx.doi.org/10.1063/1.4944640>]

Over the past decade, high-order harmonic generation (HHG) from laser-ablated plume (LAP) has attracted considerable attention,^{1–4} since it is a promising technique to develop intense tabletop coherent sources of extreme ultraviolet (XUV) radiation.^{5–8} Using this technique, several types of solid targets have been used for HHG, and intense harmonics have been demonstrated from numerous materials.^{8,9} In the LAP technique, one efficient method to generate intense XUV pulses is to use resonant harmonics (RH). In several laser-ablated media, RHs are generated due to the perturbation of the HHG process by resonant autoionizing states, resulting in significant enhancement in the harmonic yield, with the energy of these RHs measured to be in the multi-micro-joule range.⁸ This energy is about one to two orders of magnitude higher compared to those generated through the conventional three-step process.⁸ The spectral bandwidth of these RHs is narrow (e.g., for RH of indium at 61.5 nm, $\Delta\lambda_{\text{FWHM}} \sim 1.2$ nm), and thus these harmonics have unique applications where narrow bandwidth XUV pulses are needed, for example, in the spectroscopy of highly charged ions¹⁰ or in coherent diffractive imaging of nanoscale objects.¹¹

In contrast, broad bandwidth high-order harmonics also have numerous applications. One application is to develop an intense attosecond laser source,^{12–14} which are promising tools to capture and control the ultrafast motion of electrons inside atoms,^{15,16} molecules,¹⁷ and solids.¹⁸ There have been extensive efforts to generate ever shorter attosecond pulses,^{19,20} and pulses as short as 67 attoseconds have been demonstrated.²¹ However, the output energy of these attosecond pulses are low^{19,22} (nano-joule range), which limits their practical applications. In order to generate intense and short attosecond pulses, one needs high-order harmonics of high photon flux and broad bandwidth. Further, intense sub-100 eV laser pulses are desirable for various applications in the field of XUV spectroscopy²³ and microscopy.²⁴

One promising method for intense and broad bandwidth harmonic generation is to use carbon plumes^{5–7} as the

nonlinear medium. In the past, we have demonstrated that high-order harmonics of multi- μJ energy are generated from carbon plumes using 0.8 μm driving laser pulses.^{5,6} By comparing the intensity of the RHs and carbon harmonics, we have shown that the intensity of each carbon harmonic order is comparable or even higher than from a single RH.²⁵

However, one disadvantage of carbon harmonics driven by 0.8 μm lasers is that its high-order harmonic cutoff is relatively low (~ 32 eV). In carbon harmonics, its high efficiency is attributed to the large photoionization cross-section of diatomic carbon molecules, which has been shown to be the major species that contribute to carbon harmonics.²⁶ However, neutral diatomic carbon molecules have relatively low ionization potential (~ 11.4 eV), resulting in the low cutoff of carbon harmonics. This low cutoff limits the applications of this intense source, such as for generating intense attosecond pulses with very short pulse duration²⁷ and other fields of XUV spectroscopy and microscopy.^{23,24}

According to the three-step model¹³ ($E_{\text{cut-off}} = I_p + 2.9 \times 10^{-13} I \lambda^2$ [eV], where I_p , I , and λ are the ionization potential, peak laser intensity, and the driving laser wavelength, respectively), the high-order harmonic cutoff can be extended by increasing the driving laser wavelength.^{28,29} However, wavelength scaling shows that in many nonlinear atomic media, the single-atom harmonics efficiency decreases rapidly (following a $\lambda^{-5} \sim -6$ scaling) as the driving laser wavelength is increased.^{30,31} This is mainly due to the quantum diffusion of the wave packet, since electrons take a longer time to propagate in the continuum.^{28,32} This effect of harmonic intensity reduction is usually compensated by improving the phase matching condition, which mainly depends on the geometry and density of the medium that is used for HHG.^{3,33,34} In gaseous media, this phase mismatch is usually overcome by using few centimeter long medium inside a hollow-core fiber, with appropriate density.^{19,35}

In this letter, we demonstrate the generation of sub-100 eV high-order harmonics with high photon flux and broad bandwidth from a thin jet ($\sim 200 \mu\text{m}$) of laser-ablated carbon molecules. We use long-wavelength driving lasers to

^{a)}ozaki@emt.inrs.ca

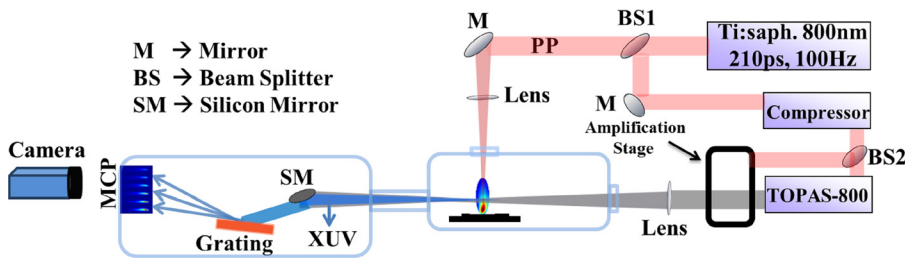


FIG. 1. Schematic diagram of the experimental setup used for the high-order harmonic generation from laser-ablated materials.

extend the cutoff and observe that high-order harmonics up to ~ 70 eV are generated with $1.71 \mu\text{m}$ driving lasers. Further, we find that the photon flux of high-order harmonics driven by $1.71 \mu\text{m}$ lasers is unexpectedly high. Experimental results show that the peak intensity of carbon high-order harmonics reduces by only about 30% when changing the driving laser wavelength from $0.8 \mu\text{m}$ to $1.71 \mu\text{m}$.

The experimental scheme used for carbon HHG is shown in Fig. 1. The experiments are performed with the 100 Hz beamline of the Advanced Laser Light Source (ALLS). This is a Ti:sapphire laser that can produce laser pulses of 80 mJ energy at $0.8 \mu\text{m}$ wavelength, with pulse duration of ~ 40 fs (~ 210 ps before compression). Graphite targets are placed inside the vacuum chamber on an XYZ translation stage under a vacuum of $\sim 10^{-5}$ Torr. To generate harmonics from solid graphite, the laser beam is divided into two beams. One part of the laser beam, named the prepulse (PP), is used to ablate a plasma plume from the solid graphite. This PP is focused on to the graphite target with a circular spot of $\sim 200 \mu\text{m}$ diameter at a PP intensity of $\sim 10^{10} \text{ W cm}^{-2}$, which results in a carbon plume that extends 1 mm from the target surface.²⁶ A fraction of the second part of the beam (~ 5 mJ) is first compressed to ~ 40 fs, and then seeded to an optical parametric amplifier (OPA; HE-TOPAS) for nonlinear frequency conversion. The output OPA energy is ~ 1 mJ at $1.8 \mu\text{m}$. This output is then subsequently amplified by an amplification stage containing a beta barium borate crystal (BBO; type II). The final output of this laser source can reach ~ 13 mJ energy in the Signal beam and ~ 10 mJ in the Idler beam. Complete details of this laser source are given elsewhere.³⁶ We use these Signal or Idler beams as the main pulse (MP), which is then focused in the nonlinear medium (i.e., the carbon ablation plume produced by the PP), after a delay of few tens of nanoseconds (ns). This delay between the PP and the MP is needed to produce neutrals in the plasma plume for maximum harmonic output, as well as to relax the electron density gradient, which would have negative effects in the HHG process. The high-order harmonics are generated collinearly with the MP, as shown in Fig. 1. This high-order harmonic beam is separated from the MP using a silicon mirror, and the reflected harmonic beam is sent to the XUV spectrometer. This spectrometer consists of a flat-field grating (Hitachi, 1200 lines/mm) and a micro-channel plate (MCP) followed by a phosphor screen. Finally, the image of the high-order harmonic spectrum is generated on the phosphor screen, and then captured by a CMOS camera (16 bit, PCO-edge).

In Fig. 2, we present the high-order harmonic spectra generated using $0.8 \mu\text{m}$ driving laser from three graphite targets, having carbon composition of 99.9% (Green; Alfa-Aesar), 97.0% (Red), and 91.0% (Blue; McMaster-Carr, Graphite-91).

In Graphite-91, the impurity is mostly 9% of oxygen, which has been confirmed using the energy dispersive X-ray spectroscopy (EDS) technique. The laser parameters, especially the PP and the MP intensities ($\sim 1.2 \times 10^{10} \text{ W cm}^{-2}$ and $\sim 2.73 \times 10^{14} \text{ W cm}^{-2}$, respectively), are kept constant to allow accurate comparison of the harmonic properties. It is observed that high-order harmonics of similar yield and cutoff are generated from these three targets. The integrated intensities per pulse of harmonics from 16 eV to 32 eV are observed as 4.8×10^7 , 5.1×10^7 , and 5.0×10^7 , from targets containing 99.9%, 97.0%, and 91.0% of carbon, respectively, and the maximum high-order harmonic cutoff is observed at ~ 32 eV. The results shown in Fig. 2 indicate that impurities in Graphite-91 have no effects on the harmonic efficiency. Therefore, we use Graphite-91 for the rest of this study, since it is less expensive.

The industrial Graphite-91 target is prepared by pressing small graphite grains at very high pressure and is used as heat-resistance material at high temperatures. We use EDS, X-ray diffraction (XRD), and scanning electron microscope (SEM) analyses to characterize this material. The EDS results (not shown here) reveal that this material contains 91% of carbon, with oxygen being the major impurity. The XRD pattern, shown in Fig. 3, shows six XRD peaks at (002), (100), (101), (004), (110), and (006), which confirms the graphitic nature of the target after compression.³⁷ Further, the grain size of this target is estimated with the high-resolution SEM image, shown in the inset of Fig. 3, which indicates that the Graphite-91 is a composite of graphite grains with sizes around 200–500 nm.

In Fig. 2, we have observed that high-order harmonics up to ~ 32 eV are generated from laser-ablated carbon molecules using $0.8 \mu\text{m}$ wavelength driving lasers. The ionization potential of the C_2 molecule is ~ 11.4 eV, and the saturation intensity is measured to be $\sim 3.64 \times 10^{14} \text{ W cm}^{-2}$. From this

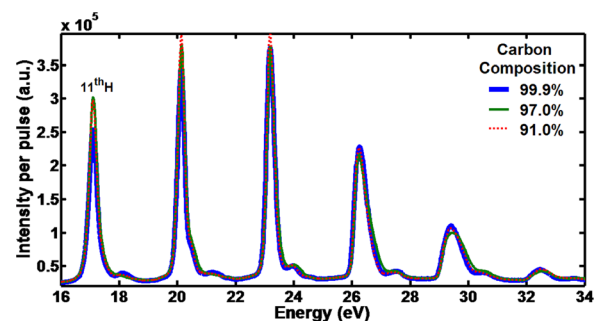


FIG. 2. High-order harmonic spectra generated using $0.8 \mu\text{m}$ driving laser from three laser-ablated graphite plumes with carbon composition of 91.0%, 97.0%, and 99.9%. High-order harmonics of similar yield and cutoff are generated from these plumes. These spectra are recorded with MP intensity of $\sim 2.73 \times 10^{14} \text{ W cm}^{-2}$.

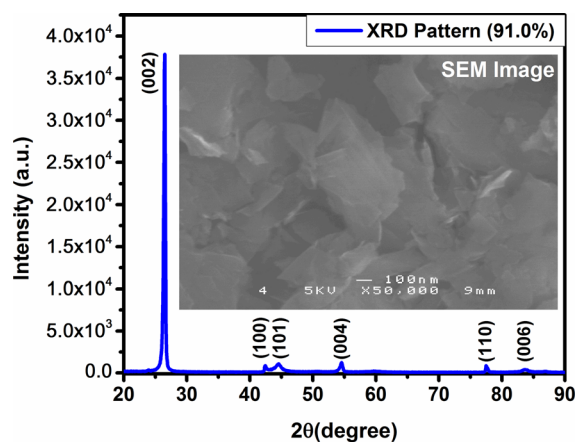


FIG. 3. XRD pattern and SEM image of Graphite-91 target. The XRD pattern shows that this target has neutral graphite structure, and the SEM image gives the graphite grain size, which is about ~ 200 – 500 nm.

ionization potential and saturation intensity, the high-order harmonic spectra in Fig. 2 indicate that harmonics are generated from neutral diatomic carbon molecules. This conclusion is also supported by our recently published results of plasma spectroscopy of the graphite ablation plume, which showed strong emission from neutral diatomic carbon molecules.²⁶

Given this relatively low cutoff of carbon harmonics driven by $0.8 \mu\text{m}$ lasers, we study carbon harmonics using long wavelength driving lasers to extend this cutoff. In Fig. 4, we show the high-order harmonic spectra generated from carbon molecules at three driving laser wavelengths, centered at $0.8 \mu\text{m}$, $1.47 \mu\text{m}$, and $1.71 \mu\text{m}$. To accurately compare the harmonic intensity, the driving laser intensity for these three wavelengths is maintained at the same value of $\sim 1.4 \times 10^{14} \text{ W cm}^{-2}$. Fig. 4(a) shows the high-order harmonic spectrum generated using driving lasers of $0.8 \mu\text{m}$ wavelength, showing a cutoff of $\sim 32 \text{ eV}$. This harmonic cutoff is further extended up to $\sim 60 \text{ eV}$ by increasing the driving laser wavelength to $1.47 \mu\text{m}$, as can be seen in Fig. 4(b). The maximum harmonic cutoff is observed with $1.71 \mu\text{m}$ laser pulses, where we have demonstrated harmonics up to $\sim 70 \text{ eV}$ (Fig. 4(c)). In fact, the configuration of our spectrometer limited the detection of harmonics up to this energy, and thus, there is a possibility that the actual harmonic cutoff with $1.71 \mu\text{m}$ laser is even higher than 70 eV .

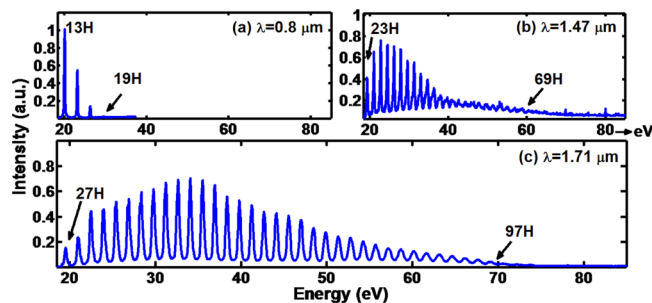


FIG. 4. High-order harmonic spectra generated from carbon molecules at driving lasers wavelength of (a) $0.8 \mu\text{m}$, (b) $1.47 \mu\text{m}$, and (c) $1.71 \mu\text{m}$. The driving laser intensity is maintained $\sim 1.4 \times 10^{14} \text{ W cm}^{-2}$ for all these spectra.

From Fig. 4, we also notice that the carbon harmonics are comparable in intensity even when using driving lasers with longer wavelength. In Fig. 4, the harmonic intensities between the three spectra can be directly compared. Using $0.8 \mu\text{m}$ driving lasers, our group has already demonstrated that high-order harmonics of multi- μJ energy with efficiencies of 2×10^{-4} for the 13th harmonic are generated from laser-ablated graphite plume.⁵ The ratio of the peak harmonic intensity for $0.8 \mu\text{m}$, $1.47 \mu\text{m}$, and $1.71 \mu\text{m}$ driving lasers is observed to be 1:0.76:0.70. This indicates that when the driving laser wavelength is changed from $0.8 \mu\text{m}$ to $1.71 \mu\text{m}$, the high-order harmonic peak intensity is reduced by only 30%, for a fixed MP laser intensity of $\sim 1.4 \times 10^{14} \text{ W cm}^{-2}$ (which is close to the saturation intensity $\sim 3.6 \times 10^{14} \text{ W cm}^{-2}$). From these results, we can estimate that conversion efficiencies of $>10^{-4}$ are obtained for carbon harmonics from 25 to 40 eV .

In conclusion, we have demonstrated that intense and broadband harmonics are generated from carbon molecules that are ablated from graphite targets. We have observed that high-order harmonics of similar properties are generated from three laser-ablated graphite plumes with different purities, showing that impurities have no effects on the harmonics efficiency. The high-order harmonic cutoff is extended by increasing the driving laser wavelength from $0.8 \mu\text{m}$ to $1.71 \mu\text{m}$. We have observed that high-order harmonics up to $\sim 70 \text{ eV}$ or higher are generated with $1.71 \mu\text{m}$ driving laser pulses. High-order harmonic spectrum shows that harmonics are intense even for driving lasers with $1.71 \mu\text{m}$ wavelength. Experimental results show that the peak harmonic intensity reduces by only $\sim 30\%$ when changing the laser wavelength from $0.8 \mu\text{m}$ to $1.71 \mu\text{m}$. This intense XUV laser source at shorter wavelengths will be a useful tool for many applications, where intense and broad bandwidth XUV pulses are required.

¹M. Suzuki, M. Baba, R. A. Ganeev, H. Kuroda, and T. Ozaki, *Opt. Lett.* **31**, 3306 (2006).

²R. A. Ganeev, M. Suzuki, M. Baba, and H. Kuroda, *Appl. Phys. Lett.* **86**, 131116 (2005).

³R. A. Ganeev, M. Suzuki, and H. Kuroda, *Phys. Rev. A* **89**, 033821 (2014).

⁴R. A. Ganeev, C. Hutchison, A. Zair, T. Witting, F. Frank, W. A. Okell, J. W. G. Tisch, and J. P. Marangos, *Opt. Express* **20**, 90 (2012).

⁵L. B. Elouga Bom, Y. Pertot, V. R. Bhardwaj, and T. Ozaki, *Opt. Express* **19**, 3077 (2011).

⁶R. A. Ganeev, L. B. Elouga Bom, J. Abdul-Hadi, M. Wong, J. Brichta, V. Bhardwaj, and T. Ozaki, *Phys. Rev. Lett.* **102**, 013903 (2009).

⁷R. A. Ganeev, T. Witting, C. Hutchison, F. Frank, P. V. Redkin, W. A. Okell, D. Y. Lei, T. Roschuk, S. A. Maier, J. P. Marangos, and J. W. G. Tisch, *Phys. Rev. A* **85**, 015807 (2012).

⁸T. Ozaki, R. A. Ganeev, M. Suzuki, and H. Kuroda, "High-Order Harmonic Generation from Low-Density Plasma" in *Advances in Solid State Lasers Development and Applications*, edited by M. Grishin (In Tech, 2010).

⁹R. A. Ganeev, *High-Order Harmonic Generation in Laser Plasma Plumes* (World Scientific, 2013).

¹⁰W. Nörtershäuser, *Hyperfine Interact.* **199**, 131 (2011).

¹¹M. D. Seaberg, D. E. Adams, E. L. Townsend, D. A. Raymondson, W. F. Schlotter, Y. Liu, C. S. Menoni, L. Rong, C.-C. Chen, J. Miao, H. C. Kapteyn, and M. M. Murnane, *Opt. Express* **19**, 22470 (2011).

¹²C. Winterfeldt, C. Spielmann, and G. Gerber, *Rev. Mod. Phys.* **80**, 117 (2008).

¹³P. Corkum, *Phys. Rev. Lett.* **71**, 1994 (1993).

¹⁴P. Corkum and F. Krausz, *Nat. Phys.* **3**, 381 (2007).

¹⁵Z. Chang, *Fundamentals of Attosecond Optics* (CRC Press, 2011).

- ¹⁶T. Popmintchev, M.-C. Chen, P. Arpin, M. M. Murnane, and H. C. Kapteyn, *Nat. Photonics* **4**, 822 (2010).
- ¹⁷G. Sansone, F. Kelkensberg, J. F. Pérez-Torres, F. Morales, M. F. Kling, W. Siu, O. Ghafur, P. Johnsson, M. Swoboda, E. Benedetti, F. Ferrari, F. Lépine, J. L. Sanz-Vicario, S. Zherebtsov, I. Znakovskaya, A. L'huillier, M. Y. Ivanov, M. Nisoli, F. Martín, and M. J. J. Vrakking, *Nature* **465**, 763 (2010).
- ¹⁸M. Schultze, K. Ramasesha, C. D. Pemmaraju, S. A. Sato, D. Whitmore, A. Gandman, J. S. Prell, L. J. Borja, D. Prendergast, K. Yabana, D. M. Neumark, and S. R. Leone, *Science* **346**, 1348 (2014).
- ¹⁹T. Popmintchev, M.-C. Chen, D. Popmintchev, P. Arpin, S. Brown, S. Alisauskas, G. Andriukaitis, T. Balciunas, O. D. Mücke, A. Pugzlys, A. Baltuska, B. Shim, S. E. Schrauth, A. Gaeta, C. Hernández-García, L. Plaja, A. Becker, A. Jaron-Becker, M. M. Murnane, and H. C. Kapteyn, *Science* **336**, 1287 (2012).
- ²⁰Z. Chang, A. Rundquist, H. Wang, M. Murnane, and H. Kapteyn, *Phys. Rev. Lett.* **79**, 2967 (1997).
- ²¹K. Zhao, Q. Zhang, M. Chini, Y. Wu, X. Wang, and Z. Chang, *Opt. Lett.* **37**, 3891 (2012).
- ²²Y. Wu, E. Cunningham, H. Zang, J. Li, M. Chini, X. Wang, Y. Wang, K. Zhao, and Z. Chang, *Appl. Phys. Lett.* **102**, 201104 (2013).
- ²³M. V. T. Schultz, *Attosecond and XUV Spectroscopy: Ultrafast Dynamics and Spectroscopy* (Wiley, 2013).
- ²⁴M. I. Stockman, M. F. Kling, U. L. F. Kleineberg, and F. Krausz, *Nat. Photonics* **1**, 539 (2007).
- ²⁵R. A. Ganeev, H. Singhal, P. A. Naik, J. A. Chakera, A. K. Srivastava, T. S. Dhami, M. P. Joshi, and P. D. Gupta, *J. Appl. Phys.* **106**, 103103 (2009).
- ²⁶M. A. Fareed, S. Mondal, Y. Pertot, and T. Ozaki, *J. Phys. B: At., Mol. Opt. Phys.* **49**, 035604 (2016).
- ²⁷M. Chini, K. Zhao, and Z. Chang, *Nat. Photonics* **8**, 178 (2014).
- ²⁸B. Shan and Z. Chang, *Phys. Rev. A* **65**, 011804 (2001).
- ²⁹B. E. Schmidt, A. D. Shiner, M. Giguère, P. Lassonde, C. A. Trallero-Herrero, J.-C. Kieffer, P. B. Corkum, D. M. Villeneuve, and F. Légaré, *J. Phys. B: At., Mol. Opt. Phys.* **45**, 074008 (2012).
- ³⁰J. Tate, T. Augustine, H. G. Muller, P. Salières, P. Agostini, and L. F. Dimauro, *Phys. Rev. Lett.* **98**, 013901 (2007).
- ³¹V. Strelkov, *Phys. Rev. Lett.* **104**, 123901 (2010).
- ³²M. Lewenstein, P. Balcou, M. Y. Ivanov, A. L'huillier, and P. B. Corkum, *Phys. Rev. A* **49**, 2117 (1994).
- ³³X. Zhang, A. L. Lytle, T. Popmintchev, X. Zhou, H. C. Kapteyn, M. M. Murnane, and O. Cohen, *Nat. Phys.* **3**, 270 (2007).
- ³⁴A. Paul, R. A. Bartels, R. Tobey, H. Green, S. Weiman, I. P. Christov, M. M. Murnane, H. C. Kapteyn, and S. Backus, *Nature* **421**, 51 (2003).
- ³⁵A. Rundquist, C. G. Durfee, Z. Chang, C. Herne, S. Backus, M. M. Murnane, and H. C. Kapteyn, *Science* **280**, 1412 (1998).
- ³⁶N. Thiré, S. Beaulieu, V. Cardin, A. Laramée, V. Wanie, B. E. Schmidt, and F. Légaré, *Appl. Phys. Lett.* **106**, 091110 (2015).
- ³⁷G. Sun, X. Li, Y. Qu, X. Wang, H. Yan, and Y. Zhang, *Mater. Lett.* **62**, 703 (2008).